Changes in the stiffness of load-bearing elements of a high-rise building and inclinometer data based on finite element analysis

Alexey Plotnikov*, and *Mikhail* Ivanov

Chuvash State University named after I.N. Ulyanov (ChSU named after I.N. Ulyanov), Moskovsky pr., 15, Cheboksary, Russia

Abstract. The use of monitoring techniques during the operation of a building contributes to the study of the stress-strain state of both known and newly developed structural systems. The article discusses the effect of reducing the bending stiffness of reinforced concrete crossbars of high-rise buildings on the overall deformability, which can be monitored by changing the angles of rotation at characteristic points. For the introduction into the model of the calculation based on finite elements of the physical parameters of the stiffness of reinforced concrete bending elements, the function of the change in the shoulder of a pair of forces in the section during the opening of normal cracks is given. Empirical data on changes in the stress unevenness coefficient along the length of the reinforcing bar are used. The calculation is based on the diagrammatic method. The data on the accumulated experience of measuring the angles of rotation of a building with automatic monitoring of buildings are presented. Using the finite element method, the systems were simulated with a decrease in stiffness to 0.4 from the initial one. It is shown that it is possible to select a range of sensors - angle meters - inclinometers. It has been determined that the angle of rotation can be changed up to 1.6 times. The corresponding ranges are defined for two types of frameworks: frame and frame-braced. The nature of the change in the overall stiffness of the building frame as a result of reducing the stiffness of the crossbars is shown. Calculation models based on the finite element method determined the deformation limits of the entire frame as a whole.

1 Introduction

Every year the "urban revolution" continues - an influx of population into large agglomerations. Vivid examples of this are cities such as Moscow, New York, Hong Kong, Chicago, Shanghai and many others. They are turning into megacities, where it is necessary to ensure the safe operation of buildings to perform their increasingly complex functions. When designing such buildings, complex engineering issues of a different nature are

* Corresponding author: plotnikovan2010@yandex.ru

solved. Spatial rigidity and general stability of a building depends not only on the geometry and rigidity of the main supporting structures constituting the system, but also on the strength of their nodal connections. The subgrade also affects the stress state of the building as a whole due to the appearance of uneven settlement and tilt.

The regularities of the operation of high-rise buildings are traditionally described by the differential equations of an elastic line - a vertical axis passing through the center of stiffness of the building in the plan. With the development of the finite element method, it became possible to obtain a picture of the deformations of such a system by numerical methods, while obtaining a similar result [1, 16, 17]. In both methods, it is possible to introduce different ratios of the stiffness parameters of horizontal and vertical load-bearing structural elements, which significantly affects the operation of the building.

During operation, due to alternating loads and destruction of materials, the rigidity of structures inevitably decreases. First of all, the accumulation of damage in the form of cracks affects, and also the flexibility of the joints increases. When examining load-bearing systems and monitoring, it is necessary to install sensors not only directly on the load-bearing elements of structures, but also in the zones of connection nodes [2-11].

One of the important parameters for observation is the rigidity of the cross-section of the crossbars, a change in which causes the flexibility of the entire supporting system, the angle of rotation on the support or near the support increases. To measure this parameter, inclinometers can be used, selecting their range based on a nonlinear computational model.

2 Materials and methods

The change in the intensity of the increase in the angles of rotation of the girders with an increase in the load, as well as the deflections, is non-linear. This is accompanied by a redistribution of efforts in the system, which is also important for assessing the bearing capacity of a building. From this point of view, the measurement of the angles of rotation is also very important [12-16].

To solve such a multistage problem, simpler methods for determining the forces in sections are needed. Usually, for this, local equations of equilibrium of forces in sections are used, written for different stages of the stress-strain state (SSS). In the standard for the calculation of SP 63.13330. by the method of limiting efforts, it is regulated at stage II to determine the shape of the compressive stress diagram as triangular, at stage III - as rectangular, in the intermediate stage - as a curved trapezoid. For the end-to-end problem, continuous functions of the dependence of the forces on the height of the compressed zone of the section of the reinforced concrete element are required.

The calculation of reinforced concrete girders, in which cracks form and develop, is carried out with the determination of geometric parameters, such as the shoulder of a pair of forces in the section, the height of the compressed zone, as well as the proportion of plastic deformations in concrete. At the stages of SSS, according to the current standards, it is necessary to take into account the three-line diagram of the operation of compressed concrete (Fig. 2).

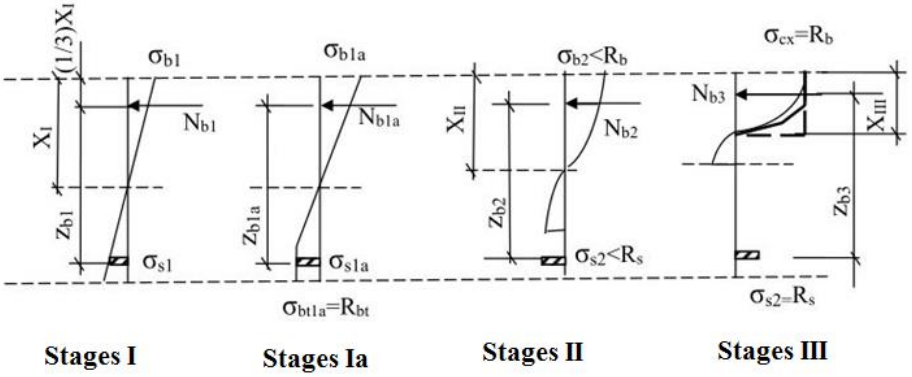

Fig. 1. Diagrams of normal stresses in the section of an element by stages of loading.

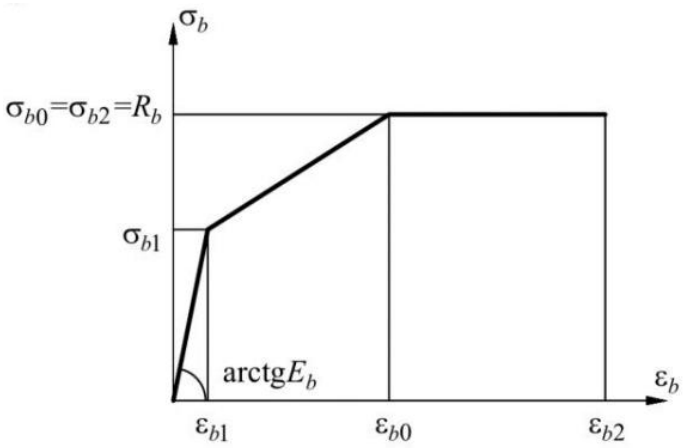

Fig. 2. Diagram of concrete deformation.

By now, considerable experience has been accumulated in describing the nonlinear operation of reinforced concrete elements. The foundations of the theory were laid by A.A. Gvozdev, a large amount of material on tests with the derivation of empirical coefficients was obtained by V.I. Murashov. Their work was developed, in particular, by V.M. Bondarenko, E.N. Kodyshem, A.G. Tamrazyan. But, in fact, the implementation of nonlinear calculations at all stages of SSS became possible with the introduction of step-by-step computer calculations [17].

To simplify the algorithm, a unified approach is needed to determine the height of the compressed zone and the arm of the pair of forces z in the section. In general, z is defined as the ratio of the static moment of the section relative to the center of gravity of the tensioned reinforcement to the reduced area of the entire section.

According to previously published data obtained by E.N. Kodyshem, A.S. Zalesov, I.K. Nikitin, L.L. By Lemysh [18], with a decrease in the relative height of the compressed zone of the section ξ by 10 - 20%, the curvature of the element 1/r will change insignificantly, since the shoulder of the pair of forces **z** in the section also changes. The sum of the deformations of compressed concrete and tensile reinforcement, and hence the curvature $\frac{1}{r} = \frac{\varepsilon_{bm}+\varepsilon_{sm}}{r}$, will change insignificantly.

Recently, on the recommendations of E.N. Kodysh, I.K. Nikitin, N.N. Trekin [18], and in the normative document SP 63.13330.2018, the shoulder of a pair of forces z is determined:

$$z = h_0 - \frac{1}{3}x_m \ . \quad (1)$$

In general, at stage II SSS, taking into account the development of the crack opening width and the growth of plastic deformations of concrete, which is expressed in a decrease in the modulus of deformations Eb, the bending stiffness is determined as:

$$D = E_{s,red}A_s z(h_0 - x_m) \quad (2)$$

где $E_{s,red} = {E_s}/{\psi_s}$ (3)

Continuous functions of bending stiffness at stages of stress-strain state are obtained by introducing a single center of rotation of the changing compressive zone of concrete relative to the center of gravity of the tensioned reinforcement. In fact, the displacement of the center of gravity of the diagram of the compressed zone relative to the tensioned reinforcement is determined between the stages of stress-strain state.

At stage II, after the formation of cracks, the material parameter $\psi_s - from\ 0.4\ to\ 1.0$ - the coefficient of stress unevenness along the length of the reinforcing bar (Fig. 3).

Non-linear analysis is usually performed by the diagrammatic method using standard relative deformations εb, with short-term and long-term loads.

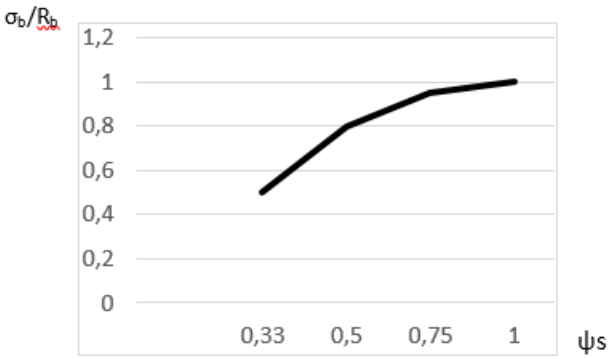

Fig. 3. The relationship between the stress level in the concrete of the compressed zone and the coefficient of stress unevenness in tensile reinforcement (according to V.I.Murashev).

$$E_{b1,red} = {0.6R_{bn}}/{\varepsilon_{b1}} \quad (4)$$

At stage II, on average:

$$E_{b0,red} = {R_{bn}}/{\varepsilon_{b0}} \quad (5)$$

At stage III:

$$E_{b2,red} = {R_{bn}}/{\varepsilon_{b2}} \quad (6)$$

Deformations that reduce the initial stiffness of the building are incorporated at the design stage, in particular for frame and frame-braced systems. The alignment of bending moments on the supports of multi-span girders is regulated, while the development of cracks in the stretched zone is allowed according to the manifestation of the properties of the plastic hinge, i.e. decrease in torque by 30%.

The effect of changing the stiffness of floor elements on the deformations of a high-rise building when changing the stiffness of the floor Bu at stage I SSS, in the situation $M_i <$

M_{crc}, at stage II under conditions $M_{crc} < M_i < M_u$, in the works of P.F. Drozdov, M.I. Dodonov [19, 20] is determined by the value:

$$s = \frac{hl^3}{12\gamma B_u b} \quad (7)$$

The value of s affects not only the general deformability of the structural system, but also the type of the elastic line of the vertical axis passing through the center of gravity of the floors.

3 Results and discussion

To assess the effect of changing the stiffness of the floors on the deformations of the bearing system, it is necessary to obtain the physical parameters of the range of stiffness that changes with increasing load, i.e. at all stages of SSS.

Such dependences with a simplified definition of the shoulder of a pair of forces z in a section at the most common value of the percentage of reinforcement of 1% were obtained in [21].

Based on the given geometric characteristics of the section at b = 150 mm, h = 350 mm, taking into account the plastic deformations of concrete in the stretched zone, which is consistent with the norms of SP 63.13330, the parameters are determined: the height of the compressed zone, the shoulder of the pair of forces z_1 = 25.4 cm. two stages by the method of projection of forces in the section, taking into account the plastic deformations of concrete in the compressed zone and the intensity of crack opening, respectively, z_2 = 25.8 cm and z_3 = 28.6 cm.

In the method of calculating the ultimate deformations of concrete and reinforcement, it is accepted to use a piecewise linear stress diagram of a compressed zone, which approximately describes a real nonlinear diagram. In this case, the height of the compressed zone:

$$x = \frac{R_{sn}A_{sn}}{\omega R_{bn} b} \quad (8)$$

After analyzing the obtained numerical values, a decision was made on the possibility of using a series of coefficients to determine the shoulder of a pair of forces z from the initial value at stage I:

β = 1-1.13 - with short-term loading,

β = 1-1.17 - with prolonged action of the load.

The amount of change in hardness B_u at stage I will be:

$$B_u = 2{,}5E_sA_sz(h_0 - x_{mI}) = 763{,}67E_sA_s \quad (9)$$

The amount of change in hardness B_u at stage III will be:

$$B_u = 2{,}5E_sA_sz(h_0 - x_{mIII}) = 665{,}1E_sA_s \quad (10)$$

The stiffness of the girder at stage I will be:

$$D = EJ = 16078125000 \text{ Н/см}^2 \quad (11)$$

The moment of inertia of the cross-section of the girder will be:

$$J = \frac{bh^3}{12} = 53593{,}8 \text{ см}^4 \quad (12)$$

The stiffness of the girder at stage III will be:

$$D = 63649600000 \text{ Н/см}^2 \quad (13)$$

In the process of cracking and the development of a plastic hinge, the bending moment in the cross-section of the girder decreases, due to a decrease in the girder stiffness at the pore by up to 2.5 times.

By specifying the physical laws of the change in the stiffness parameters of the sections, it is possible to simulate the total stress-strain state of the entire bearing system using computer programs such as Lira-CAD, SCAD OFFICE and others.

Experience shows that the modeling of the work of reinforced concrete with cracks in such programs has not yet been implemented. Changing the stiffness parameters of nodal connections in the support sections of the girders can be introduced by the introduction of reduced values of the deformation modulus within the reduction of the support moment to 30%.

Due to the change in stiffness during operation, it is also relevant when setting restrictive parameters (settings) for unique buildings to track the angles of rotation in a nonlinear relationship [22]. The finite element method considers the range of stiffness reduction to 0.4 from the initial one. Thus, it is possible to select the range of angle meters - inclinometers.

If inclinometers are installed through ¼ of the building height [23, 24], especially at the crossbar-column junction, deformations of the vertical axis of the elastic line can be obtained. The greater the deviation of the column from the vertical, the more likely the formation and development of cracks in the joints. Cracks, in turn, also increase the angle of rotation of the entire structure. The general angle of rotation of the girder-column assembly consists of several components:

$$\varphi = \varphi_1 + \varphi_2 + \Delta\varphi \quad (14)$$

где φ_1 – extreme column angle, φ_2 – swing angle of the middle column, $\Delta\varphi$ – additional angle of rotation, depending on the width of the crack opening in structures

To analyze the development of deformations in the systems, two calculation models of the frame and frame-braced frame of a high-rise building were collected. Changes in the support moment and the angle of rotation of the girder structure were taken at the crossbar-column intersection nodes, horizontally in a group at 6 points through ¼ of the building height (Fig. 4).

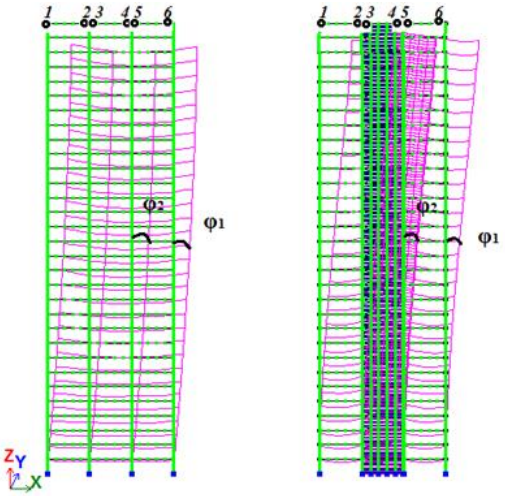

Fig. 4. Frame and frame-braced building frameworks.

For the presented bearing systems, in flat fragments, the range of stiffness reduction from 1.0 to 0.4 of the initial parameters of the bending stiffness of the girder was considered.

For all design solutions, the range of stiffness reduction to 0.4 of the initial parameters of the beam structure stiffness was considered.

Table 1. Summary of bending moments in the cross-section of the transom for the frame building frameworks.

x/H	benchmark	Bending moment in the cross-section of the girder, kN/m					
		1	2	3	4	5	6
E= 2,942·10^7 kN/m^2							
0	0	-103.15	-826.535	-299.565	-798.083	-259.043	-778.965
1/4	24.5	-552.743	-411.352	-243.806	-737.426	36.9466	-1063.32
1/2	52.5	-889.3	-95.0329	-288.938	-624.824	171.132	-1174.83
3/4	80.5	-1107.64	103.258	-364.503	-517.495	197.25	-1183.3
1	105	-831.417	-26.2551	-403.476	-395.855	-99.6748	-746.748
E= 2,3536·10^7 kN/m^2							
0	0	-105.829	-789.339	-271.738	-771.983	-233.57	-761.259
1/4	24.5	-521.842	-406.224	-225.417	-718.761	45.1355	-1029.64
1/2	52.5	-847.966	-100.098	-275.7	-609.533	168.778	-1132.84
3/4	80.5	-1062.86	95.5623	-352.752	-504.465	190.577	-1138.78
1	105	-818.707	-12.3096	-388.433	-379.908	-84.0069	-734.359
E= 1,1768·10^7 kN/m^2							
0	0	-108.959	-678.046	-196.049	-684.046	-165.156	-690.679
1/4	24.5	-411.933	-399.684	-166.561	-659.159	61.3307	-910.832
1/2	52.5	-698.228	-131.406	-232.691	-559.618	145.776	-981.701
3/4	80.5	-897.233	51.4549	-315.188	-461.131	149.877	-975.511
1	105	-755.646	-8.9663	-349.215	-336.607	-56.4373	-674.48

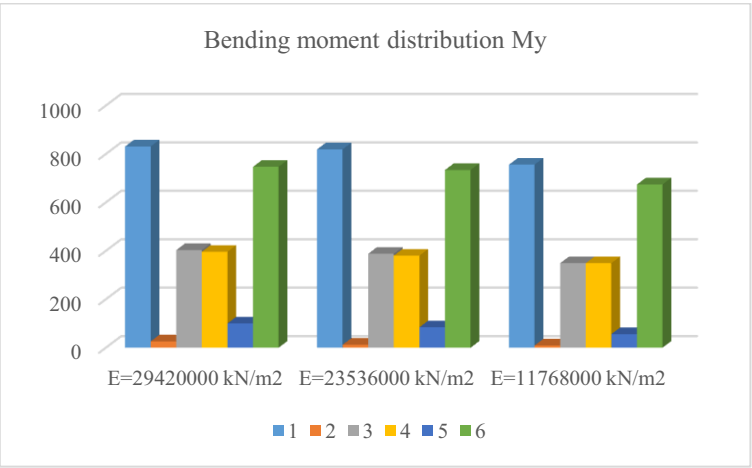

Fig. 6. Diagram of the distribution of the bending moment in the support section of the girder for the frame building frameworks at elev. 105 m.

Table 2. Summary of bending moments in cross-sections of the girder span for a frame building frameworks.

x/H	benchmark	Bending moment in cross-sections of the girder span, kN/m		
		1 span	2 span	3 span
E= 2,942·10^7 kN/m^2				
1	105	464.233	416.411	452.99
E= 2,3536·10^7 kN/m^2				
1	105	477.699	416.411	452.99
E= 1,1768·10^7 kN/m^2				
1	105	515.178	472.708	508.076

Table 3. Angles of rotation in the supporting sections of the frame girder for the frame building frameworks.

x/H	benchmark	Angle of rotation uY in the cross-section of the girder, rad * 1000					
		1	2	3	4	5	6
E= 2,942·10^7 kN/m^2							
0	0	1.31183	0.310037	0.542432	0.340296	0.558201	0.066282
1/4	24.5	1.67247	0.752719	0.887259	0.11482	0.261187	-0.22968
1/2	52.5	1.81636	0.930448	1.00799	-0.11044	-0.014228	-0.59155
3/4	80.5	1.77686	0.947455	1.44988	-0.29346	-0.224767	-0.88502
1	105	2.52102	1.01407	1.10021	-0.61264	-0.510591	-1.92701
E= 2,3536·10^7 kN/m^2							
0	0	1.4127	0.37986	0.653678	0.396099	0.655357	0.343383
1/4	24.5	1.75735	0.813322	0.975567	0.184329	0.360375	-0.15144
1/2	52.5	1.87394	0.967895	1.06286	-0.06137	0.0554867	-0.54099
3/4	80.5	1.80938	0.961424	1.02461	-0.2695	-0.185389	-0.86377
1	105	2.57791	1.03886	1.13914	-0.64827	-0.528096	-1.97572
E= 1,1768·10^7 kN/m^2							
0	0	1.82584	0.698528	1.15017	0.680979	1.1197	0.470823
1/4	24.5	2.19749	1.12652	1.4182	0.533869	0.84677	0.219175
1/2	52.5	2.17942	1.15968	1.34455	0.178836	0.397882	-0.30931
3/4	80.5	1.98628	1.0304	1.16117	-0.15508	0.0107108	-0.77551
1	105	2.78781	1.10277	1.27268	-0.76042	-0.556395	-2.14618

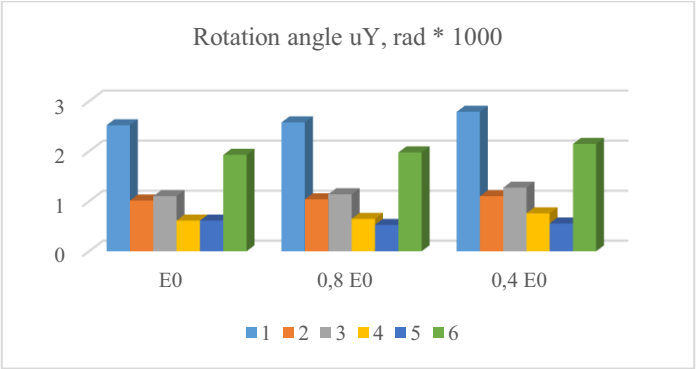

Fig. 7. Diagram of the angles of rotation in the cross-section of the cross-section of the transom for the frame building frameworks at elev. 105 m.

Table 4. Summary of bending moments in the cross-section of the girder for the frame-braced building frameworks.

x/H	benchmark	Bending moment in the cross-section of the girder, kN/m					
		1	2	3	4	5	6
E= 2,942·10^7 kN/m^2							
0	0	0	69.0035	0	-11.5373	0	69.0035
1/4	24.5	0	69.0035	0	-9.77494	0	69.0035
1/2	52.5	0	69.0035	0	-9.86414	0	69.0035
3/4	80.5	0	69.0035	0	-9.95347	0	69.0035
1	105	0	69.0035	0	-9.81228	0	69.0035
E= 2,3536·10^7 kN/m^2							
0	0	0	69.0035	0	-11.3073	0	69.0035
1/4	24.5	0	69.0035	0	-9.76421	0	69.0035
1/2	52.5	0	69.0035	0	-9.92337	0	69.0035
3/4	80.5	0	69.0035	0	-10.0827	0	69.0035
1	105	0	69.0035	0	-9.84865	0	69.0035
E= 1,1768·10^7 kN/m^2							
0	0	0	69.0035	0	-11.0414	0	69.0035

1/4	24.5	0	69.0035	0	-9.99932	0	69.0035
1/2	52.5	0	69.0035	0	-10.2468	0	69.0035
3/4	80.5	0	69.0035	0	-10.4944	0	69.0035
1	105	0	69.0035	0	-9.88064	0	69.0035

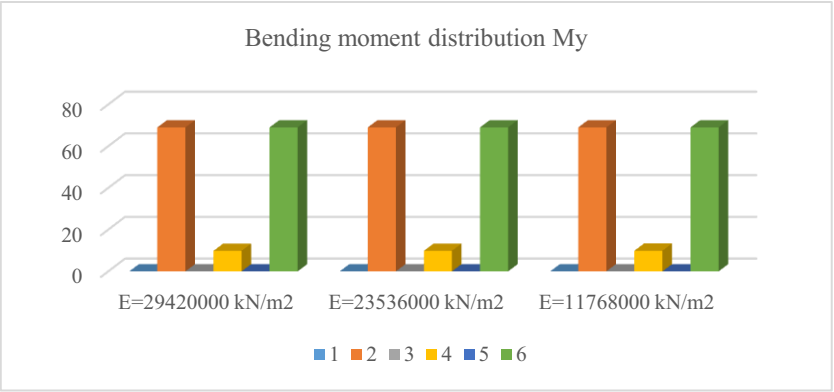

Fig. 8. Diagram of the distribution of the bending moment in the cross-section of the girder for the frame-braced building frameworks at elev. 105 m.

Table. 5. Summary of bending moments in the cross-sections of the girder span for the frame-braced building frameworks.

x/H	benchmark	Bending moment in cross-sections of the girder span, kN/m		
		1 span	2 span	3 span
E= 2,942·10^7 kN/m^2				
1	105	880.147	-29.8428	880.147
E= 2,3536·10^7 kN/m^2				
1	105	880.147	-29.8428	880.147
E= 1,1768·10^7 kN/m^2				
1	105	880.147	-29.8428	880.147

Table 6. Summary of the angles of rotation in the cross-section of the crossbar for the frame-braced building frameworks.

x/H	benchmark	Angle of rotation uY in the cross-section of the girder, rad * 1000					
		1	2	3	4	5	6
E= 2,942·10^7 kN/m^2							
0	0	2.78553	-3.18363	0.105694	0.180775	3.04603	-2.92314
1/4	24.5	1.60516	-4.364	0.85779	0.886496	3.49498	-2.47418
1/2	52.5	0.715219	-5.25395	1.29528	1.32435	3.94529	-2.02388
3/4	80.5	0.241612	-5.72755	1.44988	1.47932	4.26215	-1.70701
1	105	0.113241	-5.85592	1.45224	1.51256	4.37061	-1.59855
E= 2,3536·10^7 kN/m^2							
0	0	-4.50704	-3.33733	0.104469	0.181231	3.19969	-3.07706
1/4	24.5	1.75951	-4.51724	0.857761	0.886235	3.64789	-2.62887
1/2	52.5	0.870011	-5.40674	1.29544	1.32431	4.09755	-2.17921
3/4	80.5	0.396677	-5.88008	1.4501	1.47937	4.41405	-1.8627
1	105	0.268409	-6.00835	1.45185	1.51303	4.52239	-1.75436
E= 1,1768·10^7 kN/m^2							
0	0	3.7087	-4.10601	0.100765	0.18199	3.96828	-3.84643
1/4	24.5	2.53005	-5.28466	0.858272	0.883827	4.4143	-3.40041
1/2	52.5	1.64184	-6.17287	1.29643	1.32253	4.86207	-2.95265
3/4	80.5	1.1693	-6.64541	1.45124	1.47787	5.17751	-2.6372
1	105	1.04134	-6.77337	1.45083	1.5128	5.28547	-2.52924

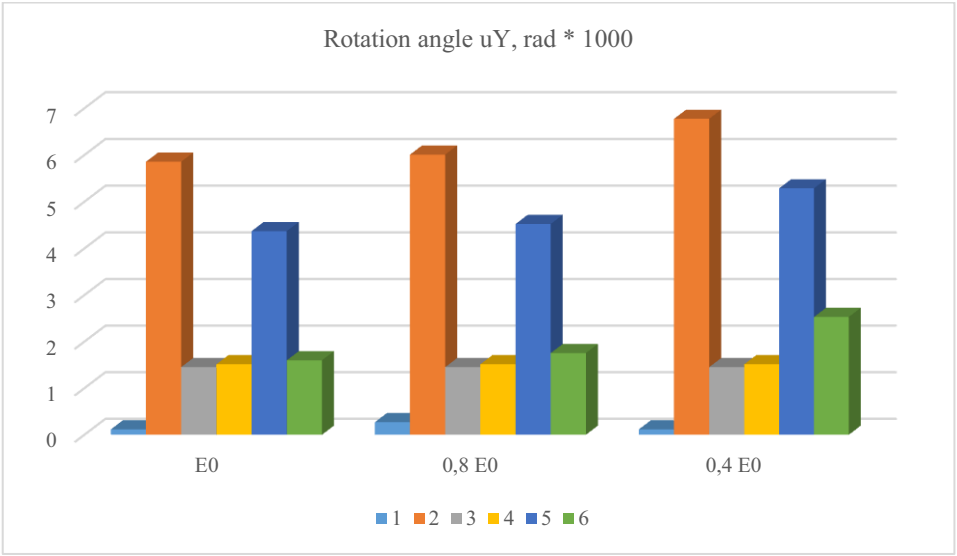

Fig. 9. Diagram of the angles of rotation in the cross-section of the girder for the frame-braced building frameworks at elev. 105 m.

Table 7. Consolidated angle of rotation in the cross-section of the girder to the frame and frame-braced building frameworks at elev. 105 m.

Frame building frameworks							
x/H	benchmark	**Angle of rotation uY in the cross-section of the girder, angle sec**					
		1	2	3	4	5	6
E= 2,942·10^7 kN/m^2							
1	105	528	209	226	126	105	397
E= 2,3536·10^7 kN/m^2							
1	105	532	214	235	134	109	408
E= 1,1768·10^7 kN/m^2							
1	105	575	228	263	157	115	443
Frame-braced building frameworks							
x/H	benchmark	**Angle of rotation uY in the cross-section of the girder, angle sec**					
		1	2	3	4	5	6
E= 2,942·10^7 kN/m^2							
1	105	23	1207	299	312	901	330
E= 2,3536·10^7 kN/m^2							
1	105	55	1239	299	312	933	362
E= 1,1768·10^7 kN/m^2							
1	105	215	1397	299	312	1090	522

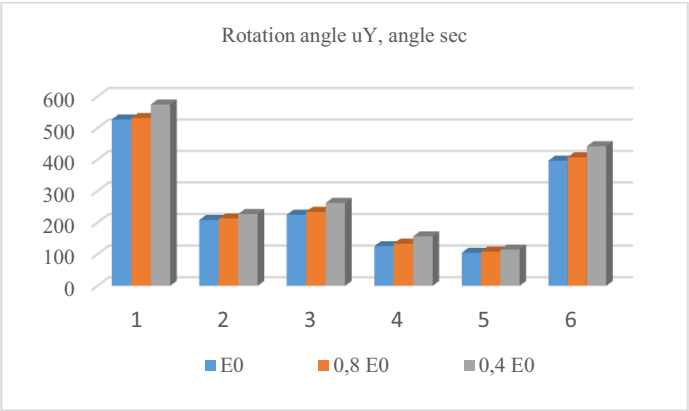

Fig. 10. Diagram of the angles of rotation in the cross-section of the cross-section of the frame building frameworks at elev. 105 m.

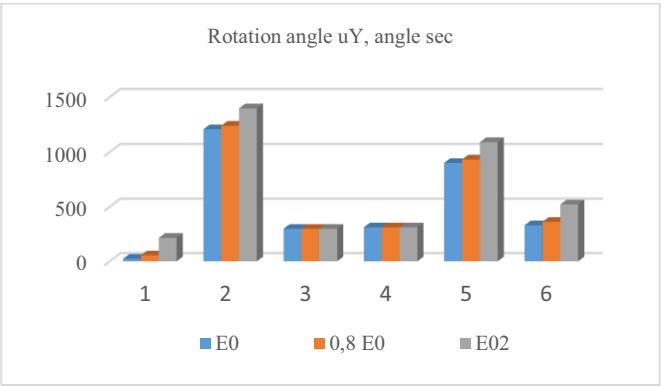

Fig. 11. Diagram of the angles of rotation in the support section of the cross-section for the frame-braced building frameworks at elev. 105 m.

Modeling was carried out by introducing low-stiffness girders in the zone of finite element nodes on a 1-m-long section. The finite element method was used to change the stiffness value from 1.0 to 0.4 from the initial one.

The decrease in the bending moment in the cross-sections of the girder span was up to 56 kN/m, the decrease in the support moment for the outer columns was up to 75 kN/m, the decrease in the support moment for the middle columns was up to 60 kN/m, which is consistent with the reduced stiffness of the horizontal elements.

With a decrease in hardness to 0.8 from the initial:

- in the nodes "crossbar - column" in the frame and frame-braced the angle of rotation increases up to 1.1 times;

With a decrease in hardness to 0.4 from the initial:

- in the nodes "girder - column" in the frame, the angle of rotation increases up to 1.2 times;
- the same, in the frame-braced frame, the angle of rotation increases up to 1.6 times.

Based on the results of the analysis of the results obtained, the angles of rotation were determined with a decrease in the supporting rigidity of the girder.

With a decrease in stiffness to 0.4 from the initial value, the difference in the angle of rotation of the frame for the extreme columns was 47 yrs. sec, for middle columns - 37 angular. sec. In the same case, for the frame-braced frame, respectively, for the extreme columns 192 angle. sec, for middle columns - 190 angular. sec.

4 Conclusions

As a result of operation, a decrease in the rigidity of reinforced concrete girders is inevitable, both from physically nonlinear processes in the girder itself, and as a result of compliance in the "girder-column" knocking zones. Hence, it is very important to measure the angles of rotation of the crossbars during automatic monitoring.

The finite element method was used to simulate various load-bearing systems in the range of stiffness reduction from 1.0 to 0.4 from the initial one. At the same time, on the basis of knowledge about the nonlinearity of the change in the stiffness of sections according to a simplified relationship to determine the shoulder of a pair of forces z, it was possible to select a range of angle sensors - inclinometers. The range of rotation angles change was obtained up to 1.6 times (up to 192 arcsec). The range is defined for two types of frames: frame and frame-braced.

With the help of inclinometers, control over the possible formation of a plastic hinge, for a decrease in stiffness in the bearing cross section of the girder is realized. According to the simulation data, the bending moment decreases to 56 kN/m in the girder span, and the supporting moment to 75 kN/m.

Using inclinometers located at a quarter of the height of the building, you can track the technical condition of not only vertical elements, but also horizontal ones, which gives more complete information about the condition of the building. It becomes necessary to develop computer programs that provide correlations of the readings of sensor groups, scenarios of the technical condition of the building. This will expand the possibilities of scientific research on various structural systems, analysis of the technical condition of buildings by the maintenance service, and more fully reveal the possibilities of integrated monitoring.

References

1. Plotnikov A.N., Ivanov M.YU., Yakovleva O.S. Zhestkostnyye parametry vysotnykh zdaniy i ikh opredeleniye pri monitoringe // Vestnik Chuvashskogo gosudarstvennogo pedagogicheskogo universiteta im. I.YA. Yakovleva. Seriya: Mekhanika predel'nogo sostoyaniya. 2020. № 1 (43). S. 55-65. (In Russian)
2. Mustafin M. G., Valkov V. A., Kazantsev A. I. Monitoring of deformation processes in buildings and structures in metropolises. Procedia Engineering. 2017. No. 189. Pp. 729-736. doi:10.1016/j.proeng.2017.05.115.
3. Yuan K., Huib Y., Chen Z. Effects of facade appurtenances on the local pressure of high-rise building. Journal of Wind Engineering and Industrial Aerodynamics. 2018. No. 178. Pp. 26-37. DOI: 10.1016/j.jweia.2018.05.004.
4. Li J, Hao H. A review of recent research advances on structural health monitoring in Western Australi // Structural Monitoring and Maintenance. 2016. № 3(1). Pp. 33-49.
5. Xiong H.-B., Cao J.-X., Zhang F.-L. Inclinometer-based method to monitor displacement of high-rise buildings // Structural Monitoring and Maintenance. 2018. № 5(1). Pp. 111-127.
6. Lee J.-J., Ho H.-N., Lee J.-H. A Vision-Based Dynamic Rotational Angle Measurement System for Large Civil Structures // Sensors. 2012. № 12(6). Pp. 7326-7336.
7. Ozbey B., Erturk V.B., Demir H.V., Altintas A., Kurc O. A Wireless Passive Sensing System for Displacement/Strain Measurement in Reinforced Concrete Members // Sensors. 2016. № 16. Pp. 479-496.

8. Ayzenkrayn Ye. Nepreryvnyy monitoring dvizheniya meridional'nykh treshchin, voznikayushchikh v obolochkakh gradiren pod vozdeystviyem vneshnikh faktorov // Stroitel'stvo unikal'nykh zdaniy i sooruzheniy. 2015. № 5(32). S. 84-94. (In Russian)
9. Belostotskiy A.M., Akimov P.A., Negrozov O.A., Petryashev N.O., Petryashev S.O., Shcherbina S.V., Kalichava D.K., Kaytukov T.B. Adaptivnyye konechnoelementnyye modeli v sistemakh monitoringa zdaniy i sooruzheniy // Inzhenerno-stroitel'nyy zhurnal. 2018. № 2(78). S. 169–178. (In Russian)
10. Hong K, Lee J, Choi SW, Kim Y, Park H.S. A strain-based load identification model for beams in building structures. // Sensors. 2013. № 13. Pp. 9909-9920.
11. Bulgakov A., Shaykhutdinov D., Gorbatenko N., Akhmedov S. Application of Full-scale Experiments for Structural Study of High-rise Buildings // Procedia Engineering. 2015. № 123. Pp. 94 – 100.
12. Plotnikov A.N. Usiliya peresekayushchikhsya izgibayemykh zhelezobetonnykh elementov pri nelineynom izmenenii zhestkosti / «Loleytovskiye chteniya – 150». Sovremennyye metody rascheta zhelezobetonnykh i kamennykh konstruktsiy po predel'nym sostoyaniyam: sbornik dokladov Mezhdunarodnoy nauchno-prakticheskoy konferentsii, posvyashchennoy 150-letiyu so dnya rozhdeniya professora, avtora metodiki rascheta zhelezobetonnykh konstruktsiy po stadii razrusheniya, osnovopolozhnika sovetskoy nauchnoy shkoly teorii zhelezobetona, osnovatelya i pervogo zaveduyushchego kafedroy zhelezobetonnykh konstruktsiy Moskovskogo inzhenerno-stroitel'nogo instituta (MISI) A.F. Loleyta. M: Izdatel'stvo MISI-MGSU. 2018. S. 346 – 350. (In Russian)
13. Golovin N.G., Plotnikov A.N. Raschet perekrestno-rebristykh perekrytiy s uchetom fizicheskoy nelineynosti / Beton i zhelezobeton – vzglyad v budushcheye: nauchnyye trudy III Vserossiyskoy (II Mezhdunarodnoy) konferentsii po betonu i zhelezobetonu (Moskva, 12-16 maya 2014 g.): v 7 t. T.1. Teoriya zhelezobetona. Zhelezobetonnyye konstruktsii. Raschet i konstruirovaniye. Moskva: MGSU, 2014, s. 234 – 244. (In Russian)
14. Tamrazyan A. G., Avetisyan L. A. Strength and bearing capacity of compressed reinforced concrete elements under dynamic loading at high temperatures. Promyshlennoe i grazhdanskoe stroitel'stvo [Industrial and Civil Engineering], 2016, no. 7, pp. 56—60. (In Russian)
15. Tamrazyan Ashot, Levon Avetisyan. “Estimation of Load Bearing Capacity of Eccentrically Compressed Reinforced Concrete Elements under Dynamic Loading in Fire Conditions.” Applied Mechanics and Materials, vol. 638–640, Trans Tech Publications, Ltd., Sept. 2014, pp. 62–65. Crossref, doi:10.4028/www.scientific.net/amm.638-640.62.
16. Ashot G. Tamrazyan,. The Assessment of Reliability of Punching Reinforced Concrete Beamless Slabs under the Influence of a Concentrated Force at High Temperatures, Procedia Engineering, Volume 153, 2016, Pages 715-720, ISSN 1877-7058, https://doi.org/10.1016/j.proeng.2016.08.231.
17. Almazov V. O., Klimov A. N. Sopostavleniye dannykh sistemy monitoringa vysotnykh zdaniy s raschetom v programmnom komplekse // Sovremennyye problemy rascheta i proyektirovaniya zhelezobetonnykh konstruktsiy mnogoetazhnykh zdaniy: sb. dokl.

Mezhdunar. nauchn. konf., posvyashch. 100-letiyu so dnya rozhdeniya P. F. Drozdova. Moskva: MGSU, 2013. S. 38–44. (In Russian)

18. Kodysh E.N, Nikitin I.K., Trekin N.N. Raschet zhelezobetonnykh konstruktsiy iz tyazhelogo betona po prochnosti, treshchinostoykosti i deformatsiyam: monografiya / E.N. Kodysh, I.K. Nikitin, N.N. Trekin. – M.: Izd-vo Assotsiatsii stroitel'nykh vuzov, 2010. – 352 s. (In Russian)
19. Drozdov P.F. Konstruirovaniye i raschet nesushchikh sistem mnogoetazhnykh zdaniy i ikh elementov. M., Stroyizdat, 1977. — 223 s. (In Russian)
20. Drozdov P.F., Dodonov M.I. i dr. Proyektirovaniye i raschet mnogoetazhnykh grazhdanskikh zdaniy i ikh elementov. M.: Stroyizdat, 1986. — 351 s. (In Russian)
21. Plotnikov A.N., Ivanova N.V. Plecho pary sil v sechenii zhelezobetonnogo izgibayemogo elementa na vsekh stadiyakh napryazhennogo sostoyaniya // V sbornike: Sovremennyye voprosy mekhaniki sploshnykh sred - 2019. Sbornik statey po materialam konferentsii s mezhdunarodnym uchastiyem. 2019. S. 52-60. (In Russian)
22. Plotnikov A.N., Levin S.A., Lukin A.G. Nikolayeva A.G., Ivanov V.A., Gonik Ye.G., Arinina N.N., Yakovleva O.S., Porfir'yeva Ye.N., Ivanov M.YU. Integral'nyy avtomaticheskiy monitoring vysotnykh, zaglublennykh i bol'sheproletnykh sooruzheniy, razrabotannyy kafedroy stroitel'nykh konstruktsiy Chuvashskogo gosuniversiteta / Novoye v arkhitekture, proyektirovanii stroitel'nykh konstruktsiy i rekonstruktsii. Materialy IV Mezhdunarodnoy (X Vserossiyskoy) konferentsii. – Cheboksary, 2018. – S. 278-294. (In Russian)
23. Plotnikov A.N., Ivanova N.V. Plecho pary sil v sechenii zhelezobetonnogo izgibayemogo elementa na vsekh stadiyakh napryazhennogo sostoyaniya // V sbornike: Sovremennyye voprosy mekhaniki sploshnykh sred - 2019. Sbornik statey po materialam konferentsii s mezhdunarodnym uchastiyem. 2019. S. 52-60. (In Russian)
24. Ivanov M.YU., Plotnikov A.N. Sistema monitoringa vysotnykh zdaniy iz printsipa minimizatsii kolichestva datchikov // Inzhenernyye kadry - budushcheye innovatsionnoy ekonomiki Rossii. 2019. № 5. S. 25-28. (In Russian)